Trial-Manufacture and Experimental Study of Particle Damping Boring Bar for Deep Hole Boring of 7075 Aluminum Alloy

HUANG Yi[1], *HAN Jianxin*[1,2*], *DONG Qingyun*[3]

1. School of Mechanical Engineering, Tianjin University of Technology and Education, Tianjin 300222, P. R. China;
2. Tianjin Key Laboratory of High Speed Cutting and Precision Machining, Tianjin 300222, P. R. China;
3. Engineering Training Center, Tianjin University of Technology and Education, Tianjin 300222, P. R. China

(Received 18 October 2024; revised 10 January 2025; accepted 16 Januany 2025)

Abstract: 7075 aluminum alloy is often used as an important load-bearing structure in aircraft industry due to its superior mechanical properties. During the process of deep hole boring, the boring bar is prone to vibrate because of its limited machining space, bad environment and large elongation induced low stiffness. To reduce vibration and improve machined surface quality, a particle damping boring bar, filled with particles in its inside damping block, is designed based on the theory of vibration control. The theoretical damping coefficient is determined, then the boring bar structure is designed and trial-manufactured. Experimental studies through impact testing show that cemented carbide particles with a diameter of 5 mm and a filling rate of 70% achieve a damping ratio of 19.386%, providing excellent vibration reduction capabilities, which may reduce the possibility of boring vibration. Then, experiments are setup to investigate its vibration reduction performance during deep hole boring of 7075 aluminum alloy. To observe more obviously, severe working conditions are adopted and carried out to acquire the time domain vibration signal of the head of the boring bar and the surface morphologies and roughness values of the workpieces. By comparing different experimental results, it is found that the designed boring bar could reduce the maximum vibration amplitude by up to 81.01% and the surface roughness value by up to 47.09% compared with the ordinary boring bar in two sets of experiments, proving that the designed boring bar can effectively reduce vibration. This study can offer certain valuable insights for the machining of this material.

Key words: 7075 aluminum alloy; boring bar; vibration reduction; particle damping

CLC number: TG713 **Document code:** A **Article ID:** 1005-1120(2025)01-0123-14

0 Introduction

7075 aluminum alloy, thanks to its superior mechanical properties of high strength and high hardness, has become an indispensable alloy material in aircraft industry. It is reported that the workload of an aircraft deep holes accounts for nearly 20% of the total[1-5]. Thus, deep hole boring in aerospace occupies a significant proportion in mechanical processing, which has become an important technical index to measure the technology progress of the aircraft industry. To be noticed, despite the above advantages of 7075 aluminum alloy, its high plasticity and ease of deformation can easily result in low machined surface and low precision of such deep hole components[6-7], leading to low production efficiency and low product percent of pass[3]. To overcome these drawbacks, it is critical and significant to improve cutting tool equipment for deep hole boring of 7075 aluminum alloy. In recent decades, boring bar with particle damping absorber has gradually attracted considerable attentions from mechanical engineering[8-9]. In our study, a particle damping boring bar, filled with various particles in its inside damping block, is designed and analyzed based on the theory of vibration control.

*Corresponding author, E-mail address: hanjianxin@tju.edu.cn.

How to cite this article: HUANG Yi, HAN Jianxin, DONG Qingyun. Trial-manufacture and experimental study of particle damping boring bar for deep hole boring of 7075 aluminum alloy[J]. Transactions of Nanjing University of Aeronautics and Astronautics, 2025,42(1):123-136.

http://dx.doi.org/10.16356/j.1005-1120.2025.01.010

Boring technique is commonly used in deep hole machining process. It requires a large extended length of boring bars. This can obviously decrease the stiffness of bars and increase the possibility of undesirable vibrations. Consequently, deep hole boring process has to face some intractable problems such as poor machining quality, rough machined surface, low processing efficiency, and severe tool wearing[10-13]. Li et al.[14] conducted a theoretical analysis and cutting experiments on the drilling model, and corrected the model coefficients under various cutting conditions, providing a theoretical basis for deep hole processing. When the length-to-diameter ratio of boring bars is greater than 5, the stiffness of bars degrades more obviously[15]. To reduce vibration, some researchers have changed the stiffness by adding different materials to the boring bar body. For example, Sortion et al.[16] replaced the entire boring bar body with hard alloy material to improve its vibration damping performance. Singaravelu et al.[17] embedded copper-based shape memory alloy in the base layer of the boring bar to achieve vibration damping. Ma et al.[18] proposed a carbon fiber reinforced shaft for machining tool systems with poor rigidity. Another effective method is to install a damper in the boring bar, which involves adding a mass-spring system to the main body[19]. For instance, Rubio et al.[20] used traditional unconstrained optimization methods to study the optimization of boring bars and derived optimized vibration damper parameters. Li et al.[21] proposed a boring bar equipped with a variable stiffness dynamic vibration absorber, which consists of vibration absorber, rubber sleeve, and damping oil. By rotating the end cover of the absorber, the whole stiffness can be adjusted. Liu et al.[22-24] proposed a boring bar with a variable mass vibration absorber inside its borehole. The stiffness of bars can be adjusted by changing the length of the telescopic beam. A concept, realizing vibration suppression via mass adjustment of the absorber, was proposed. In a word, vibration damping boring bars using dynamic absorbers have been gradually used in machining process due to the ease of use and maintenance, and their obvious vibration reduction performances. However, the main drawback of current damping boring bars is the relatively narrow bandwidth of vibration absorption. Moreover, it seems to be difficult to realize real-time adjustment[8]. Therefore, innovative design on absorber attracts so many attentions, which promotes the development of cutting tool equipment.

As is known, the particle damping technology is a new type of vibration control method. Damping particles are often placed at a position where the vibration of main structure is intense, or along the vibration transmission path of the structure. When the main structure vibrates, damping particles collide and rub against each other. This can dissipate energy of the vibration system and achieve vibration reduction. Vibration absorption via particle damping has the advantages of high durability, high reliability, and low sensitivity for temperature[25-27], among which the greatest one is the ability to directly absorb kinetic energy, exhibiting high damping performances. Traditional vibration absorbers can only transfer system energy rather than dissipating, which may lead to high-frequency harmonic vibration[28]. Sanchez et al.[29] utilized frequency-response functions to study the mass and damping ratio of particle dampers. They found that the maximum value is not the same as before when the gap is different between the container and particles. In fact, it is actually greater than the sum of the mass of the container and particles. Zhang et al.[30] combined the advantages of classical dynamic vibration absorbers to design a new type of damping device tuned particle dampers(TPDs). They established equivalent theoretical models to describe the behavior of the cantilever system after TPD treatment. Currently, the particle damping technology is widely utilized in the vibration reduction of boring bars[31-33]. Guo et al.[34] proposed a novel type of variable stiffness TPDs for boring bar vibration reduction. Biju et al.[35] introduced high-carbon steel spherical particles into the empty cavities at the tip of a boring bar and proposed a boring bar based on particle impact. The impact of adding particles was analyzed through the surface morphology, surface roughness, and roundness of the workpiece. It was found that the radial vibration of the boring bar had a significant impact on the surface morphology of the workpiece. Chockalingam et al.[36] mixed Cu and Zn particles and filled

them into the inner cavity of a boring bar. Experiment showed a 55% reduction of the amplitude of the boring bar and 80% reduction of the surface roughness of the workpiece, significantly enhancing the stability of the boring process.

The above results indicate the superiority of vibration-reducing boring bars to traditional boring methods. However, when difficult-to-machine and high-processing-standard material comes, deep hole machining process has to face many unavoidable challenges. Although traditional vibration dampers applied in boring bars has significant contributions on vibration suppression, the vibration-damping equipment can work only when the vibration of boring process is within the range of the natural frequency of the vibration dampers. When resonant frequency is irregular, it fails to work. To be noticed, particle damping has the advantage of realizing the adaptive control of the frequency bandwidth of the vibration dampers[22]. Generally, damping particles are designed to reduce vibration through direct colliding with the main body of boring bar. These behaviors may increase the possibility of collision-induced vibration between particle damping and boring bar. To avoid this, this paper proposes a modified structure design of a particle damping boring bar. It can enable the vibration-damping range to cover the range of vibration frequencies, thereby enhancing the effectiveness of vibration suppression during drilling operations.

1 Design Procedure

Based on the existing results on vibration reduction via particle damping, we intend to dig a cavity inside the damping block. It can avoid direct collision between particle damping and boring bar. The following is the detailed design procedure.

1.1 Theoretical design

Based on the theory of vibration control, a conceptional damping boring bar system shown in Fig.1 (a) can be simplified as a two-degree-of-freedom (2-DOF) model which consists of a main bar structure and a vibration damping system as shown Fig.1(b). m_1 and k_1 are the mass and the stiffness of the main system, respectively. m_2 is the shock absorber mass; k_2 the absorber spring stiffness; c the damping coefficient of the rubber support; and $F\sin(\omega t)$ the exciting force applied to the main system.

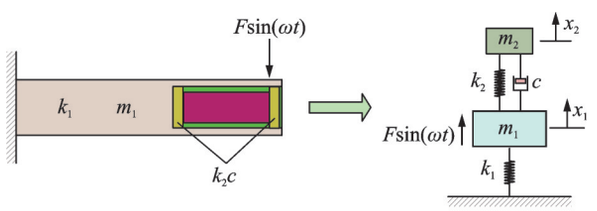

(a) Conceptional damping boring bar system (b) 2-DOF model

Fig.1 Dynamic model

The dynamic equation of motion of this 2-DOF model can be given by

$$\begin{bmatrix} m_1 & 0 \\ 0 & m_2 \end{bmatrix}\begin{pmatrix} \ddot{x}_1 \\ \ddot{x}_2 \end{pmatrix}+\begin{bmatrix} c & -c \\ -c & c \end{bmatrix}\begin{pmatrix} \dot{x}_1 \\ \dot{x}_2 \end{pmatrix}+\begin{bmatrix} k_1+k_2 & -k_2 \\ -k_2 & k_2 \end{bmatrix}\begin{pmatrix} x_1 \\ x_2 \end{pmatrix}=\begin{pmatrix} F \\ 0 \end{pmatrix}\sin(\omega t) \tag{1}$$

In order to better understand the relationship between the main system and the added (particle damping) system, we define

$$B_0=\frac{F}{k_1},\ p_1=\sqrt{\frac{k_1}{m_1}},\ p_2=\sqrt{\frac{k_2}{m_2}},\ \mu=\frac{m_2}{m_1},\ \alpha=\frac{p_2}{p_1},\ \zeta=\frac{c}{2p_1m_2},\ \lambda=\frac{\omega}{p_1} \tag{2}$$

where B_0 is the static deformation; p_1 the natural frequency of the main system; p_2 the natural frequency of the absorber system; μ the mass ratio; α the frequency ratio; and ζ the damping ratio. Then, the dimensionless amplitude ratio can be given by

$$\frac{B_1}{B_0}=\sqrt{\frac{(\lambda^2-\alpha^2)^2+(2\zeta\lambda)^2}{[\mu\lambda^2\alpha^2-(\lambda^2-1)(\lambda^2-\alpha^2)]^2+(2\zeta\lambda)^2(\lambda^2-1+\mu\lambda^2)^2}} \tag{3}$$

When the natural frequency of the shock absorber is equal to the working frequency of the main system, the vibration of the main system will be eliminated. This phenomenon is called anti-resonance.

Taking $\mu=0.05$ and $\alpha=1$ as an example, and we obtain the amplitude-frequency response curves

of this system, as depicted in Fig.2. Fig.2 shows that when the damping ratio is equal to 0, it is similar to the undamped shock absorber; when the damping ratio is too large, the system becomes a single degree of freedom system. In the process of developing a damping dynamic shock absorber, the key lies in selecting the appropriate m_2 and k_2. The purpose of this is to ensure that the amplitude is consistent at the two intersection points of the curve, that is, the tangent to the curve at these two intersection points is horizontal. Then in a fairly wide frequency range, the main system has vibration less than the allowable amplitude, which achieves the purpose of reducing the vibration of the main system.

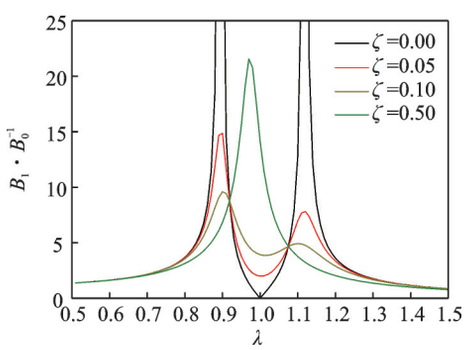

Fig.2 Amplitude-frequency response curves: $\alpha=1$, $\mu=0.05$

Through the above theoretical analysis, the design procedures of the particle damping boring bar are as follows.

(1) According to m_1 and p_1, the mass of the vibration absorber can be determined according to the cavity size of the boring bar and the material of the damping block. Then, the mass ratio can be determined.

(2) Then it comes to determine the frequency ratio $\alpha=\dfrac{p_2}{p_1}=\dfrac{1}{1+\mu}$ and calculate the absorber spring stiffness $k_2=m_2 p_2^2$.

(3) The damping ratio is calculated as $\zeta=\sqrt{\dfrac{3\mu}{8(1+\mu)^3}}$ and the damping coefficient of rubber support is $c=2\zeta m_2\omega_2$.

If the boring bar elastic modulus $E=2.11\times10^{11}$, density $\rho=7\,850\ \mathrm{kg/m^3}$, we can obtain $m_1=2.160\ 09$ kg, $k_1=9.860\ 97\times10^6$ N/m and $p_1=340.015$ Hz.

According to the above steps, the followings can be calculated: The shock absorber mass $m_2=0.108$ kg, the absorber spring stiffness $k_2=1.727\ 73\times10^5$ N/m, and the damping coefficient of rubber support $c=9.122$.

1.2 Structural design

We conducted an extensive study on the available damping boring bars on the market and consider the actual production needs, then design a granular damping boring bar based on the common market boring bar HC40-LBK4-400L. The particle damping boring bar is composed of ten parts, as shown in Fig.3. The mass block, rubber support and particle damping form a particle damping dynamic absorber. The particle damping absorber is loaded into the cavity of the boring bar. A cavity damping block is designed to place particles. The internal particles are blocked with a thread plug. The rubber support sleeve is placed on the steps at both ends of the mass block to form a complete particle damping dynamic shock absorber. The followings are the detailed design procedures.

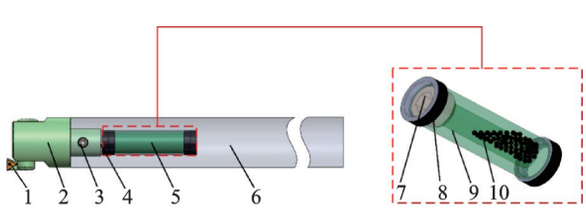

1—Cutting tool; 2—Boring head; 3—Top wire; 4—Gaskets; 5—Particle damped power vibration dampers; 6—Boring bar; 7— Thread plugging; 8—Rubber support; 9—Cavity damping block; 10—Particle damping

Fig.3 Schematic diagram of particle damping dynamic damping boring bar

(1) Boring bar

The dynamic stiffness is determined by the static stiffness and the damping is generated by the tool rod. Taking out the cavity on the boring bar can inevitably cause the loss of the static stiffness of the tool bar. However, due to the effect of rubber support and internal particles, the static stiffness loss will be compensated by the damping. For the parti-

cle damping absorber, the more particles are involved in the cavity, the better the vibration reduction performance. Therefore, to design the cavity of the boring bar, we should try to increase the size of the cavity as much as possible while ensuring that the static stiffness is not lost too much. In this case, the total length of the boring bar is 400 mm and the diameter is 40 mm. The cavity length is 100 mm and the diameter is 20 mm.

(2) Particle damper

To obtain good performance, the material of the damping block should give priority to the material with high density. The density of tungsten-based alloy is as high as 18.3 g/cm^3, and the impact strength is 10—30 J/cm^3. In addition, the tungsten-based heavy alloy has good machinability and can be conventionally machined. Therefore, we choose tungsten-based alloy as the design material of vibration damping block. Besides, to reduce the vibration amplitude of the main system, the mass of the shock absorber should be as large as possible. Therefore, the necessary parts for positioning or sealing are removed in the cavity of the boring bar, and the remaining space is left to the damping block. Therefore, the length of the damping block is 65 mm, the diameter is 18 mm, and there are steps of 2.5 mm long and 1 mm high at both ends to place the rubber support.

(3) Rubber support

The radial deformation of the rubber ring under load is nonlinear, but the deformation is small and negligible. The inner diameter is 16 mm and the outer diameter is 20 mm. The rubber spring is installed at both ends of the damping block, and its length is set to 5 mm according to the size of the damping block.

2 Damping Ratio Analysis

2.1 Data acquisition

In order to assess the damping performance of the particle damper within the boring bar, a modal impact test is conducted. The test takes into account various particle materials, particle diameters, and filling ratios. Through these experiments, the optimal filling parameters for the particle damper in the boring bar are determined.

The utilized experimental signal acquisition system is the LMS SCADAS. For the excitation of metal materials in the experiment, a hammer with a sensitivity of 0.21 mV/N is employed as the excitation device. An acceleration sensor from PCB Piezotronics in the United States is selected, with the model number SERIAL #38260 and a sensitivity of 99.6 mV/g. The computer acquisition software is the Simcenter Test.Lab data analysis software, which is a processing tool for the acquisition and analysis of vibration, noise, and other signal data.

Experiments with different fillers are conducted in the cavity at the front end of the boring bar. An impact hammer is used to strike the boring bar, while an acceleration sensor is attached to the corresponding position on the opposite side of the hammering point. This acceleration sensor captures the frequency response signal of the boring bar and transmits it to the LMS vibration and noise test and analysis system. Subsequently, the test results are thoroughly analyzed and processed using data analysis software on a computer, as shown in Fig.4.

The experimental data is meticulously analyzed and refined through the Simcenter Test.Lab software, which is designed to work in tandem with the LMS vibration measurement system. By employing the modal analysis capabilities of the Time MDOF module within the software, the first-order damping ratio is determined, with the corresponding experimental data presented in Table 1. The findings reveal an enhancement in the first-order damping ratio across various filling parameters when compared to ordinary boring bar, a clear indication of the damping effect in action. Notably, the use of 5 mm cemented carbide balls has yielded the optimal outcome, with a damping ratio of 19.386%, representing a significant improvement over ordinary boring bar. The vibration damping performance of the boring bar also lies in the parameters of the damping particles. In the followings, we analyze the damping particles material, diameter, fill rate change on the vibration characteristics of the boring bar.

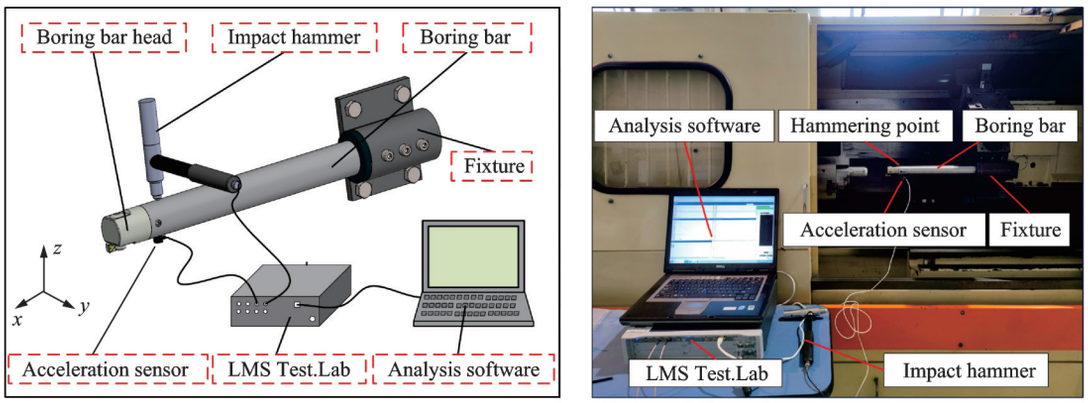

(a) Schematic diagram (b) Experiment field diagram

Fig.4 Schematic diagram of hammering experiment

Table 1 The first-order damping ratio of boring bar with different filling parameters

Filling material	Fill rate /%		
	50	70	90
Aluminum ball (1 mm)	4.900	10.658	4.740
Aluminum ball (3 mm)	6.120	8.252	5.780
Aluminum ball (5 mm)	4.275	9.757	7.287
Steel powders	10.940	12.938	7.479
Steel ball (3 mm)	14.230	15.842	6.294
Steel ball (5 mm)	10.637	13.157	4.934
Carbide powders	3.750	8.093	7.657
Carbide ball (3 mm)	10.480	12.161	9.333
Carbide ball (5 mm)	12.361	19.386	14.312

2.2 Particles effects

(1) Particle materials

A case with a diameter of 5 mm and 70% fill rate is selected. The frequency and time domain comparisons of the damping of particles for different materials are shown in Fig.5. It is observed from that the carbide balls possess the smallest amplitude and the fastest decay rate in the time domain, followed by the steel balls and finally the aluminum balls. Since denser particles carry more energy and kinetic energy during movement, and cemented carbide exhibits superior elastic properties compared to aluminum and iron, with higher restitution coefficients, the frequency of particle collisions increases, leading to greater energy dissipation.

(2) Particle diameter

Fig.6 illustrates the damping ratio bar chart for particles of different diameters at various fill rates. In Fig.6(a), the damping ratio for aluminum particles increases as the particle size decreases, with

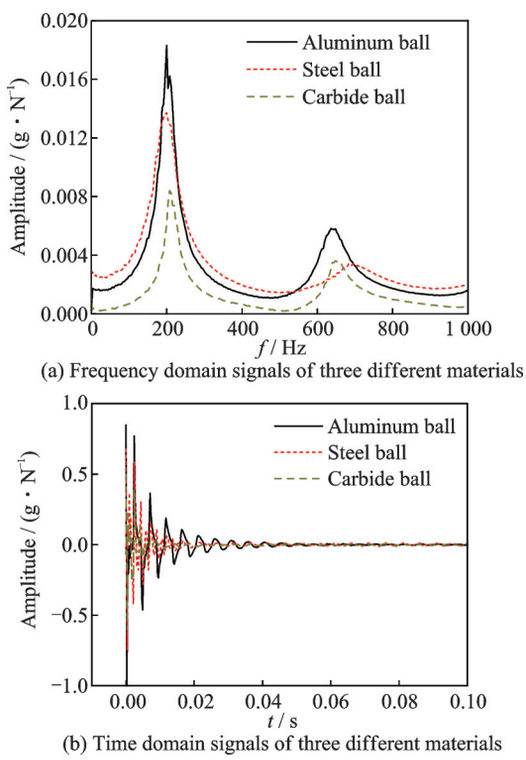

(a) Frequency domain signals of three different materials

(b) Time domain signals of three different materials

Fig.5 Comparison of frequency domain and time domain of different material particles

1 mm particles exhibiting the highest damping ratio, followed by 3 mm, and 5 mm showing the lowest. This trend can be attributed to the lower density of aluminum. Under identical impact conditions, the smaller 1 mm particles, owing to their higher collision frequency, dissipate more energy, resulting in the observed order of 1 mm > 3 mm > 5 mm. In Fig.6(b), the damping ratio for steel particles is the highest for 3 mm balls, followed by the powdered steel, and the lowest for 5 mm balls. Steel has a moderate density and elastic performance. However, under the same filling rate, pow-

dered steel tends to accumulate partially and does not fully engage in collisional energy dissipation. In contrast, there are more 3 mm steel balls than 5 mm balls, meaning a greater number of particles participate in collisions, thus consuming more energy. Fig.6(c) shows that for cemented carbide particles, the damping ratio is the highest for 5 mm particles, followed by 3 mm, and the lowest for powdered particles. At the same filling rate, the total mass of the filling material decreases in the order of powder, 3 mm, and 5 mm. Due to the high density of cemented carbide, powdered and 3 mm particles are more prone to accumulate, which is less effective than 5 mm particles in achieving more collisions at a moderate particle count, thereby enhancing energy dissipation.

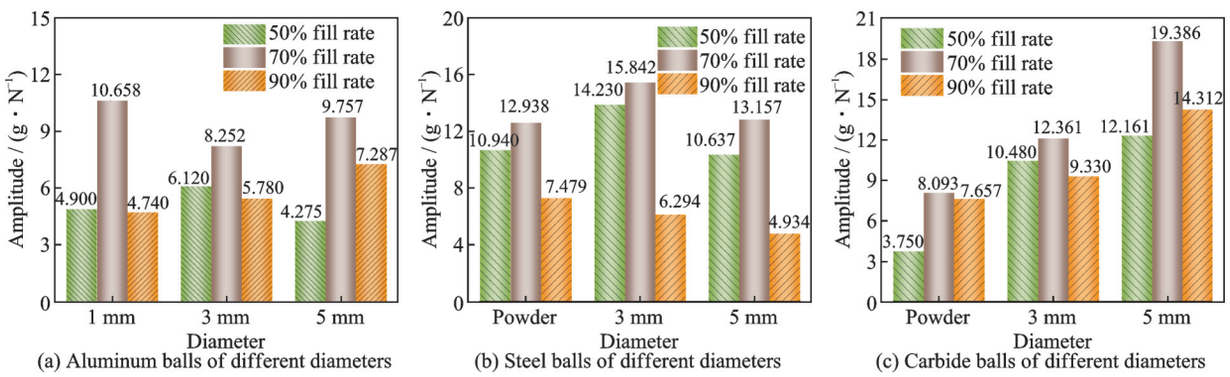

Fig.6 Columnar diagrams of damping ratio of damping particles with different diameters

(3) Fill rate

The experiments have revealed that the damping ratio initially increases with the rise of the fill rate and then decreases after reaching a peak. The optimal damping ratio, and consequently the best vibration damping effect, are achieved at a filling rate of 70%, as demonstrated in Fig.7. At a 50% filling rate, the limited number of particles reduces collisions with the chamber walls and among the particles themselves, resulting in inadequate energy dissipation. Conversely, at a filling rate of 90%, the particles are too closely packed, offering little space for movement, and tend to accumulate under the influence of gravity, which decreases the collision frequency and reduces the energy absorption capacity of the particles as a result. A filling rate of 70% provides the optimal vibration damping effect, as the vibration energy is primarily dissipated through collisions and friction among the particles and between the particles and the container walls. At a filling rate of 70%, there are enough particles and sufficient space in the container to ensure the occurrence of collisions and friction, thereby ensuring the consumption of vibration energy.

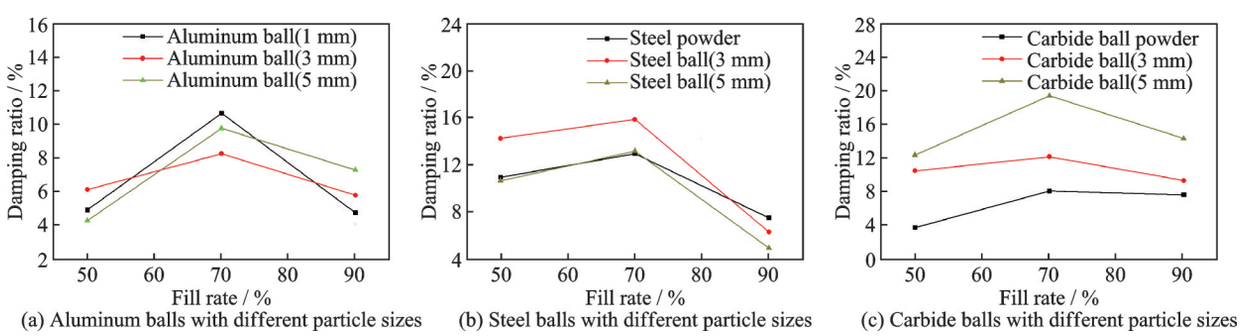

Fig.7 Diaphragms of damping ratio of damping particles with different filling rates

The results of the modal test indicate that the best damping effect of the boring bar is achieved when filled with 5 mm diameter cemented carbide balls at a filling rate of 70%. To further verify the performance of this configuration in an actual machining environment, boring experiments with 7075

aluminum alloy material are planned. This experiment will assess the boring bar's ability to control vibrations, ensuring that its damping effect is equally effective in industrial applications.

3 Cutting Experiment

3.1 Experimental setup

The properties of the material can have a certain impact on the machining effect[37-38]. The material used in the experiment is 7075 aluminum alloy, whose physical properties are shown in Table 2, and chemical composition is shown in Table 3. The 7075 aluminum alloy bars purchased from the market, after T6 heat treatment, possess good comprehensive properties, including high strength, good toughness, and certain corrosion resistance[39-40]. The bars are then machined into workpieces with an outer diameter of 65 mm, an inner diameter of 45 mm, and a height of 45 mm. When clamping the boring bar, the length-to-diameter ratio is maintained at 9∶1, and the maximum boring depth is 360 mm. To ensure the accuracy and consistency of the experiment, the vibration measurement system employs the same signal acquisition system used in the modal test, including identical acceleration sensors and other equipment. The position of the acceleration sensor is also consistent with that used in the modal test. Fig.8 shows the schematic diagram of the experimental setup.

Table 2 Main physical properties of 7075 aluminum alloy

Tensile strength/ MPa	0.2% yield strength/ MPa	Elastic modulus/ GPa	Hardness/ HB	Density/ ($g \cdot cm^{-3}$)	Poisson's ratio
524	455	71	150	2.81	0.33

Table 3 Chemical composition of 7075 aluminum alloy

%

Si	Fe	Cu	Mn	Mg	Cr	Zn	Ti
0.4	0.5	1.2—2.0	0.3	2.1—2.9	0.18—0.28	5.1—6.1	0.2

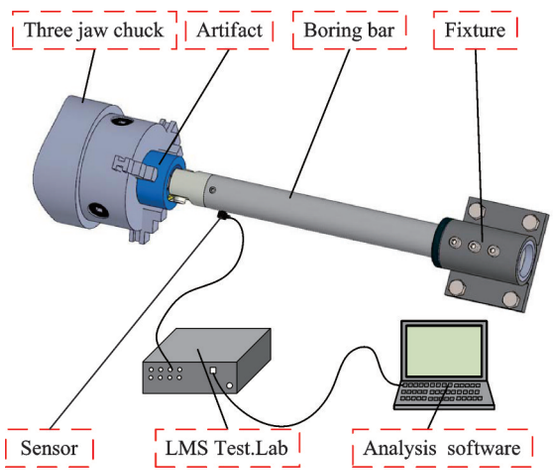

Fig.8 Principal diagram of cutting experiment

3.2 Experimental scheme and process

The single factor experiment is used to study the vibration reduction performance of the vibration reduction boring bar. The experimental parameters are shown in Table 4. In order to make the experimental results more obvious, the experiment adopts larger cutting parameters, which is convenient for collecting vibration signals and comparing the results.

During the experiment, the boring bar and the workpiece are clamped on the machine tool fixture and the three-jaw chuck respectively, the vibration

Table 4 Cutting experiment scheme

Number	Working condition	Cutting speed/($r \cdot min^{-1}$)	Feedrate/($mm \cdot r^{-1}$)	Cutting depth/mm
1	No vibration reduction	500	0.5	0.7
2	No vibration reduction	700	0.5	0.7
3	Carbide(powder)70%	500	0.5	0.7
4	Carbide ball(3 mm)70%	500	0.5	0.7
5	Carbide ball(5 mm)70%	500	0.5	0.7
6	Carbide ball(5 mm)70%	700	0.5	0.7
7	Carbide ball(5 mm)70%	300	0.5	0.7
8	Carbide ball(5 mm)50%	700	0.5	0.7
9	Carbide ball(5 mm)90%	700	0.5	0.7
10	Steel ball(5 mm)70%	700	0.5	0.7

measurement system is connected, and the sensor is pasted on the front end of the boring bar. The data analysis software is debugged, and the acceleration vibration time domain diagram is collected. The sampling time is 10 s. After completion, the program is written on the CNC lathe according to the experimental parameters, and the cutting and vibration signals of the workpiece are collected in turn according to the experimental order. The test site is shown in Fig.9.

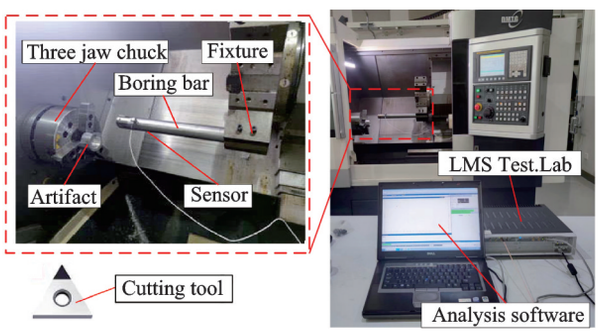

Fig.9 Cutting experiment site

3.3 Experimental results

After the experiment is completed, the vibration data from the workpiece during cutting is captured using the Signature Acquisition module in LMS Test.Lab. The data is extracted and graphically analyzed. Employing the two-sided peak detection method, the mean amplitude of the workpiece's vibration is calculated, along with the extraction of the maximum amplitude value, as shown in Table 5. Given that an acceleration sensor is used in the experiment, the results are presented as acceleration amplitudes with the unit of g/N. It should be noted that since the acceleration sensor measures in the direction of $-Z$ axis, the amplitude values are negative.

Table 5 Maximum amplitude and average amplitude

g/N

Number	Maximum amplitude	Average amplitude
1	−7.629	−3.646
2	−6.671	−3.882
3	−4.949	−3.097
4	−3.769	−1.477
5	−2.000	−0.706
6	−2.246	−0.737
7	−1.746	−0.612
8	−6.432	−3.124
9	−4.560	−1.654
10	−5.215	−2.306

Subsequently, the surface quality of the workpiece serves as a direct reflection of the experimental results. A white light interferometer is used to measure the surface topography and surface roughness. First, a small section of the workpiece is cut off. Second, measurements are taken at three different locations. Finally, the average value is taken. The workpiece is placed horizontally along the direction of the cutting speed, as shown in Fig.10.

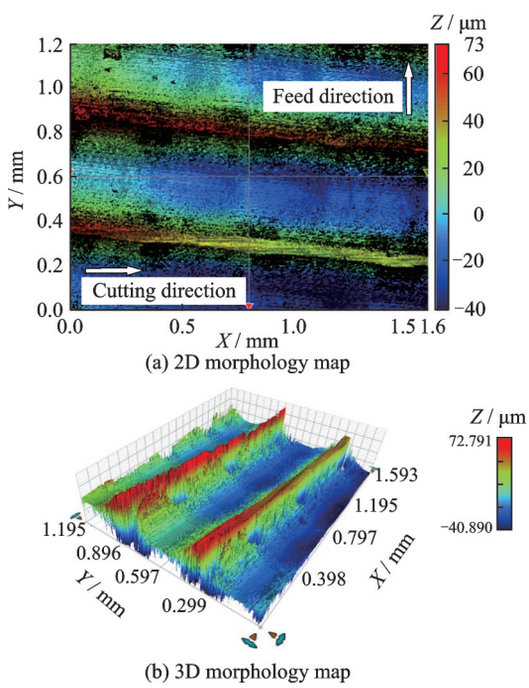

Fig.10 Surface morphology of the workpiece measured by the white light interferometer

To evaluate the performance of the developed damping boring bar in deep-hole machining of 7075 aluminum alloy, experiments 1, 2, 5, 6 are conducted. Experiments 1 and 2 utilize conventional boring bars with different cutting speeds. Experiments 5 and 6 employ damping boring bars with corresponding cutting speeds matching those of experiments 1 and 2, respectively. Fig.11(a) displays the time-domain vibration signals recorded during these experiments. The average amplitude results in Fig.12 show that the signal amplitudes in experiments 5 and 6, which use the damping boring bar,

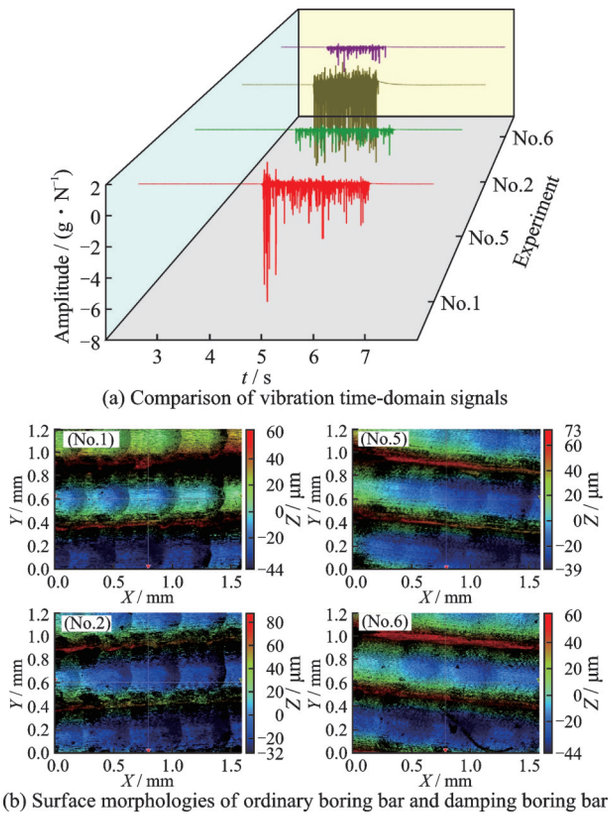

(a) Comparison of vibration time-domain signals

(b) Surface morphologies of ordinary boring bar and damping boring bar

Fig.11 Test result comparison graph

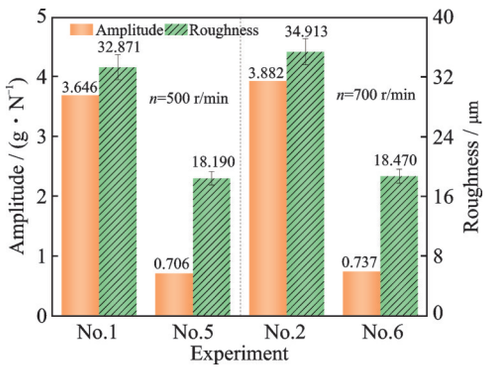

Fig.12 Comparison of average vibration amplitude and workpiece roughness between ordinary boring bar and damping boring bar

have significantly decreased. Specifically, under the same cutting conditions, the average time-domain signal amplitude for experiment 1 is −3.646 g/N, while for experiment 5 it is reduced to −0.706 g/N, showing a reduction of 80.64%. Similarly, under identical cutting conditions, the average amplitude for experiment 6 is 81.01%, lower than that for experiment 2. Fig.11(b) displays the surface imagery of the workpieces, as captured by a white light interferometer. The workpieces from experiments 1 and 2, which are machined without the use of a damping boring bar, exhibit significant fluctuations in the cutting marks. In contrast, the surfaces of the workpieces from experiments 5 and 6, where a damping boring bar is employed, are noticeably smoother. This contrast further corroborates the effectiveness of the damping boring bar in the machining process. Fig.12 presents a comparison of the surface roughness values among the workpieces from the four experiments, indicating that the workpieces machined with the damping boring bar have achieved lower surface roughness values.

Due to the strong nonlinear characteristics of particle damping, the verification of the filling parameters of particle damping in modal test may not be fully applicable to the actual processing, so we also need to analyze and verify the damping boring bar under different filling parameters in boring processing.

To investigate the effects of damping particles made from different materials on the vibrations of a boring bar, experiments 6 and 10 are specifically designed. Experiment 6 utilizes a 70% filling rate of 5 mm cemented carbide balls, whereas experiment 10 employs a 70% filling rate of 5 mm steel balls. Fig.13(a) displays the comparative time-domain vibration signals for both experiments, highlighting significant differences. The average amplitude of vibrations in experiment 6 is measured at 0.737 g/N, while experiment 10 records a higher amplitude of 2.306 g/N, reflecting a reduction of 68.04% in experiment 6. Fig.13(b) presents the surface roughness comparison, where experiment 10 shows a roughness value of 26.644 μm, and experiment 6 exhibits a superior surface finish at 18.19 μm, which is 26.19% lower than that of experiment 10. These results emphasize the superior damping performance and the positive impact on surface finish quality when using cemented carbide balls in comparison to steel balls during the boring operation.

In all respects, the particle damping and vibration reduction performance of cemented carbide material is superior to that of steel material. This once again confirms the analysis of damping with different material particles observed in modal testing.

For analyzing the performance of cutting exper-

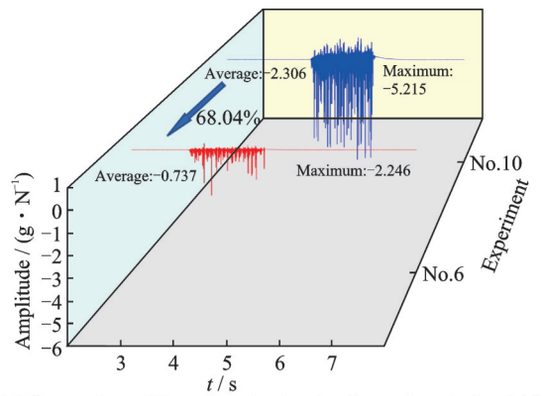

(a) Comparison of time-domain signals of experiments 6 and 10

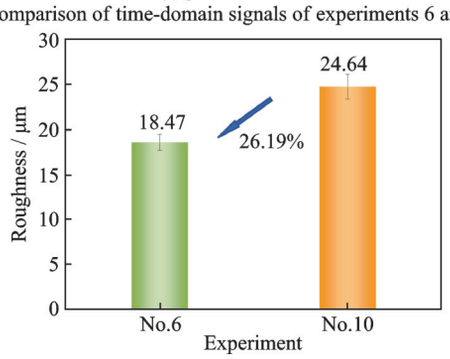

(b) Comparison of workpiece roughness in experiments 6 and 10

Fig.13 Text results of different materials

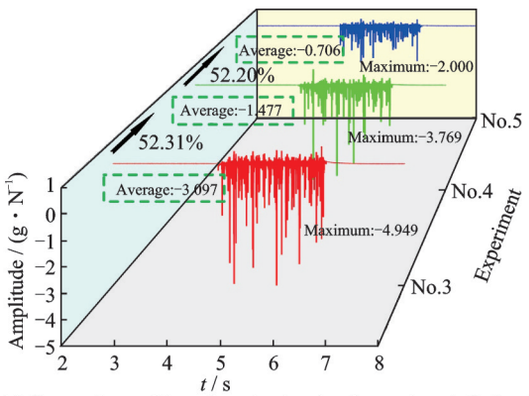

(a) Comparison of time-domain signals of experiments 3, 4 and 5

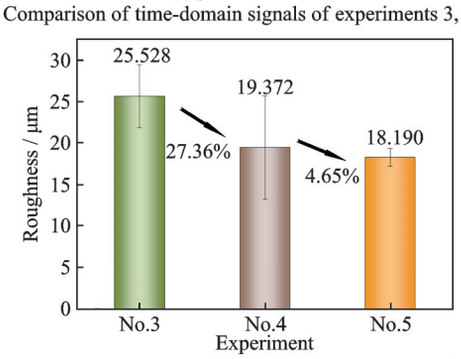

(b) Comparison of workpiece roughness in experiments 3, 4 and 5

Fig.14 Text results of different particle sizes

iments with different particle sizes, experiments 3, 4, and 5 are designed, all with a 70% filling rate. Specifically, experiment 3 utilizes cemented carbide powder, experiment 4 uses 3 mm cemented carbide balls, and experiment 5 employs 5 mm cemented carbide balls. By comparing the time-domain signals of experiments 3, 4, and 5 presented in Fig.14(a), it is observed that as the particle size increases, both the average and maximum vibration amplitudes significantly decrease. In terms of specific experimental data, experiment 3 shows a 52.31% reduction in vibration amplitude compared to experiment 4, and experiment 4 exhibits a 52.2% reduction in vibration amplitude compared to experiment 5. Upon further observation of the workpiece roughness comparison in Fig.14(b), it can be seen that the workpiece roughness for experiments 3, 4, and 5 are 25.048, 19.371, and 18.47 μm, respectively, showing a trend of decreasing by 27.36% and 4.65% in succession.

These experimental data clearly demonstrate that the vibration damping effect of using 5 mm cemented carbide balls is significantly superior to that of 3 mm cemented carbide balls, which in turn is more effective than using cemented carbide powder. This pattern is consistent with the analysis of damping by different material particles in modal testing.

To explore the impact of different filling rates on the performance of cutting experiments, we conducts experiments 8, 6, and 9 using 5 mm cemented carbide balls at filling rates of 50%, 70%, and 90%, respectively. Fig.15(a) illustrates the comparison of time-domain signals measured under these three filling rates, presenting both the average and maximum amplitudes of the vibration signals. It is observed that as the filling rate increases, the average and maximum vibration amplitudes exhibits a trend of decreasing initially and then increasing. Notably, at the 70% filling rate, the vibration signal amplitude is minimized, with an average reduction of 76.41% compared to that at the 50% filling rate and 55.44% compared to that at the 90% filling rate. Fig.15(b) presents a comparison of the workpiece surface roughness. The surface roughness of the workpieces at filling rates of 50%, 70%, and 90% are 25.677, 18.19, and 21.235 μm, respectively. It is evident that the best surface quality is achieved at the 70% filling rate.

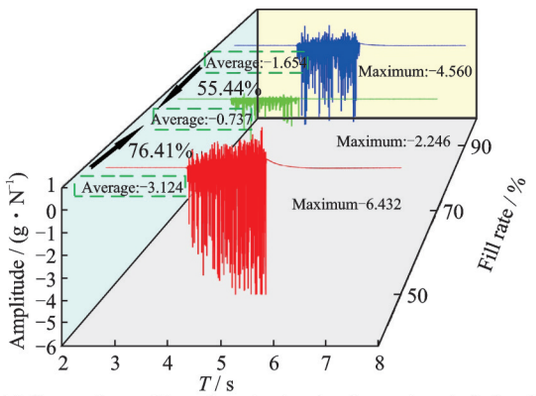

(a) Comparison of time-domain signals of experiments 8, 6 and 9

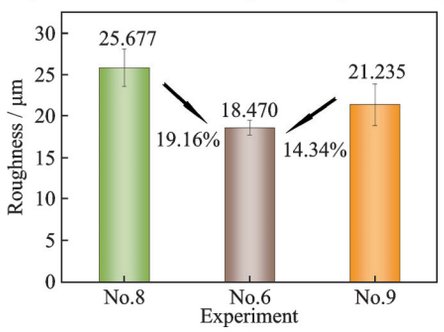

(b) Comparison of workpiece roughness in experiments 8, 6 and 9

Fig.15 Test results of different filling rates

These cutting experiments have once again confirmed that the damping boring bar with particle damping exhibits optimal vibration reduction effects at the 70% filling rate. This finding is consistent with the modal testing analysis and further validates the potential and effectiveness of particle damping technology in vibration control applications.

4 Conclusions

This paper has completed the trial production of a particle damping dynamic vibration reduction boring bar through theoretical analysis and parameter calculation. Through modal testing and cutting experiments, the excellent vibration reduction performance of the boring bar in deep-hole processing of 7075 aluminum alloy has been verified, and the following conclusions can be drawn.

(1) When using 70% filling rate of 5 mm diameter cemented carbide particles for particle damping, the vibration reduction effect is superior to that under other conditions.

(2) The designed vibration reduction boring bar can reduce the maximum processing vibration amplitude by up to 81.01%, and the surface roughness value can be reduced by up to 47.09% compared to the ordinary boring bar.

In summary, the designed particle damping dynamic vibration reduction boring bar has shown significant vibration reduction effects in the deep-hole boring process of 7075 aluminum alloy, providing strong technical support and reference for the deep-hole machining of this material.

Reference

[1] YANG Z C, ZHU L D, ZHANG G X, et al. Review of ultrasonic vibration-assisted machining in advanced materials[J]. International Journal of Machine Tools and Manufacture, 2020, 156: 103594.

[2] KUMAR S, KUMAR D, SINGH I, et al. An insight into ultrasonic vibration assisted conventional manufacturing processes: A comprehensive review[J]. Advances in Mechanical Engineering, 2022, 14(6): 16878132221107812.

[3] DUAN Z J, LI C H, DING W F, et al. Milling force model for aviation aluminum alloy: Academic insight and perspective analysis[J]. Chinese Journal of Mechanical Engineering, 2021, 34(1): 1-35.

[4] YANG S K, TONG J L, LIU Z Q, et al. Experiental study on the roundness of deep holes in 7075 aluminum alloy parts by two-dimensional ultrasonic elliptical vibration boring[J]. Micromachines, 2023, 14(12): 2185.

[5] BIERMANN D, BLEICHER F, HEISEL U, et al. Deep hole drilling[J]. CIRP Annals, 2018, 67(2): 673-694.

[6] ZHOU B, LIU B, ZHANG S G. The advancement of 7XXX series aluminum alloys for aircraft structures: A review[J]. Metals, 2021, 11(5): 718.

[7] BOUZEKOVA-PENKOVA A, MITEVA A. Some aerospace applications of 7075 (B95) aluminium alloy[J]. Aerospace Research in Bulgaria, 2022, 34: 165-179.

[8] LEE N, LIU X Y, WANG J S. Structural design and vibration analysis of the built-in damping boring bar [C]//Proceedings of 2018 International Conference on Computational, Modeling, Simulation and Mathematical Statistics (CMSMS 2018). [S.l.]: [s.n.], 2018.

[9] SRINIVASAN R, SYATH ABUTHAKEER S, JOHN PETER SOOSAIRAJ S, et al. Experimental study on minimization of boring bar vibration and surface roughness of the workpiece using viscoelastic particle damping[J]. International Journal of Manufacturing Technology and Management, 2016. DOI:

10.1504/ijmtm.2016.10005268.

[10] LIU Qiang. Research progress on vibration control of vibration reduction boring bars[J]. Journal of Jilin University (Engineering Edition), 2023, 53(8): 2165-2184. (in Chinese)

[11] LI Yuan. Research on boring bar design based on working deformation analysis[J]. Mechanical Research and Application, 2014, 27(2): 17-19.(in Chinese)

[12] YIGIT U, CIGEROGLU E, BUDAK E. Chatter reduction in boring process by using piezoelectric shunt damping with experimental verification[J]. Mechanical Systems and Signal Processing, 2017, 94: 312-321.

[13] BIJU C V, SHUMUGAM M S. Development of a boring bar with magneto rheological fluid damping and assessment of its dynamic characteristics[J]. Journal of Vibration and Control, 2018, 24(14): 3094-3106.

[14] LI L, HE N, WU P, et al. A gun drill mechanics model analysis based on 15-5PH solid solution stainless steel[J]. Machining Science and Technology, 2019, 23(2): 218-231.

[15] GUO Y J, DONG H Y, WANG G F, et al. Vibration analysis and suppression in robotic boring process[J]. International Journal of Machine Tools and Manufacture, 2016, 101: 102-110.

[16] SORTION M, TOTIS G, PROSPERI F. Modeling the dynamic properties of conventional and high-damping boring bars[J]. Mechanical Systems and Signal Processing, 2013, 34(1/2): 340-352.

[17] SINGARAVELU C, VARATHARAJAN P, RAMU G, et al. Investigation of damping characteristics on copper-based shape memory alloy frictional damper in boring process[J]. Arabian Journal for Science and Engineering, 2021, 21(6): 501-512.

[18] MA Z, CAI C Y, YIN Y K, et al. Vibration characteristics and machining performance of carbon fiber reinforced shaft in poor rigidity machining tool system[J]. The International Journal of Advanced Manufacturing Technology, 2024, 134(5): 2637-2652.

[19] SHI Jianfen. Safety basin erosion and bifurcation of a two-degree-of-freedom damped boring bar system[J]. Vibration and Shock, 2018, 37(22): 238-244.(in Chinese)

[20] RUBIO L, LOYA J A, MIGUELEZ M H, et al. Optimization of passive vibration absorbers to reduce chatter in boring[J]. Mechanical Systems and Signal Processing, 2013, 41(1/2): 691-704.

[21] LI L, SUN B B, HUA H T. Analysis of the vibration characteristics of a boring bar with a variable stiffness dynamic vibration absorber[J]. Shock and Vibration, 2019, 1: 5284194.

[22] LIU X L, LIU Q, WU S, et al. Analysis of the vibration characteristics and adjustment method of boring bar with a variable stiffness vibration absorber[J]. The International Journal of Advanced Manufacturing Technology, 2018, 98(1): 95-105.

[23] LIU Qiang. Study on vibration reduction performance of variable mass dynamic vibration absorber boring bar[J]. Journal of Harbin University of Science and Technology, 2018, 23(5): 25-29.(in Chinese)

[24] LIU X L, LIU Q, WU S, et al. Research on the performance of damping boring bar with a variable stiffness dynamic vibration absorber[J]. The International Journal of Advanced Manufacturing Technology, 2017, 89(9): 2893-2906.

[25] YAN Weiming. Parameter optimization method and effectiveness evaluation of frequency modulated particle damper[J]. Journal of Vibration and Shock, 2016, 35(7): 145-151. (in Chinese)

[26] LU Zheng. Review of particle damping technology[J]. Journal of Vibration and Shock, 2013, 32(7): 1-7.(in Chinese)

[27] DU Yanchen, ZHANG Minging. Theory and experiment of collision damping with particle damper[J]. Aerodynamics, 2012, 27(4): 789-794. (in Chinese)

[28] YAO Bing. Experimental study on particle damping vibration absorber[J]. Journal of Vibration Engineering, 2014, 27(2): 201-207. (in Chinese)

[29] SANCHEZ M, PUGNALONI L A. Effective mass overshoot in single degree of freedom mechanical systems with a particle damper[J]. Journal of Sound and Vibration, 2011, 330(24): 5812-5819.

[30] ZHANG K, XI Y H, CHEN T N, et al. Experimental studies of tuned particle damper: Design and characterization[J]. Mechanical Systems and Signal Processing, 2018, 99: 219-228.

[31] AFSHARFARD A, FARSHIDIANFAR A. Free vibration analysis of nonlinear resilient impact dampers[J]. Nonlinear Dynamics, 2013, 73(1): 155-166.

[32] WAGHMARE P J, PATIL R V, WAGHMARE G S. A review on vibration mitigation of boring bar using passive damping techniques[J]. International Journal of Research in Engineering and Technology, 2015, 4(7): 138-141.

[33] SUYAMA D I, DINIZ A E, PEDERIVA R. The use of carbide and particle-damped bars to increase tool overhang in the internal turning of hardened steel[J]. The International Journal of Advanced Manufacturing Technology, 2016, 86(5): 2083-2092.

[34] GUO X Y, ZHU Y N, LUO Z, et al. Variable stiffness tuned particle dampers for vibration control of cantilever boring bars[J]. Applied Mathematics and Mechanics, 2023, 44(12): 2163-2186.
[35] BIJU C V, SHUNMUGAM M S. Investigation into effect of particle impact damping (PID) on surface topography in boring operation[J]. The International Journal of Advanced Manufacturing Technology, 2014, 75(5): 1219-1231.
[36] CHOCKALINGAM S, NATARAJAN U, GEORGE CYRIL A. Damping investigation in boring bar using hybrid copper-zinc particles[J]. Journal of Vibration and Control, 2017, 23(13): 2128-2134.
[37] ZHANG L, LI W L, WANG Y Z, et al. The influence of milling process parameters on the low-cycle fatigue life of nickel-based powder superalloy at 650 ℃[J]. Transactions of Nanjing University of Aeronautics and Astronautics, 2023, 40(5): 511-521.
[38] WANG J, JIANG W G, HU C X. Effect of TiB_2 nanoparticles on microstructure and mechanical properties of $Ni_{60}Cr_{21}Fe_{19}$ alloy in rapid directional solidification process: Molecular dynamics study[J]. Transactions of Nanjing University of Aeronautics and Astronautics, 2024, 41(5): 575-588.
[39] DANG J Q, WANG H H, WANG C G, et al. Microstructure evolution and surface strengthening behavior of 300 M ultrahigh strength steel under engineered surface treatments[J]. Materials Characterization, 2024, 215: 114127.
[40] DANG J Q, LI Y G, ZHANG X X, et al. Surface fatigue characterization and its enhancement by the engineered ultrasonic rolling process for 300 M ultrahigh strength steel[J]. Theoretical and Applied Fracture Mechanics, 2024, 134: 104707.

Acknowledgement This work was supported by the Scientific Research Program of Tianjin Education Committee (No.2022ZD030).

Authors

The first author Mr. **HUANG Yi** received the B.S. degree in mechanical manufacture and automation from Tianjin University of Technology and Education, Tianjin, China, in 2022. He is currently pursuing the M.S. degree in mechanical engineering. His research interests are vibration analysis and control of boring bar.

The corresponding author Dr. **HAN Jianxin** received the Ph.D. degree in engineering mechanics from Tianjin University, Tianjin, China, in 2016. Since 2016, he has been affiliated with School of Mechanical Engineering, Tianjin University of Technology and Education, where he is currently an associate professor. His research has focused on linear and nonlinear vibration and control of mechanical systems.

Author contributions Mr. **HUANG Yi** complied the models, conducted the analysis, interpreted the results and wrote the manuscript. Dr. **HAN Jianxin** contributed to the scientific idea and the financial support. Mr. **DONG Qingyun** contributed to the experimental design, data acquisition and analysis. All authors commented on the manuscript draft and approved the submission.

Competing interests The authors declare no competing interests.

(Production Editors: XU Chengting, WANG Jie)

基于7075铝合金深孔镗削的颗粒阻尼减振镗杆试制与实验研究

黄 仪[1], 韩建鑫[1,2], 董庆运[3]

(1.天津职业技术师范大学机械工程学院, 天津 300222, 中国;2.天津市高速切削与精密加工重点实验室, 天津 300222, 中国;3.天津职业技术师范大学工程实训中心, 天津 300222, 中国)

摘要:7075铝合金因其优越的力学性能,常被用作航空工业中的重要承力结构。在深孔镗削过程中,由于加工空间有限、环境恶劣以及大伸长率导致刚度低,镗杆容易振动。为了减少振动、提高加工表面质量,基于振动控制理论设计了一种内部阻尼块填充颗粒的颗粒阻尼镗杆。然后确定了理论阻尼系数,设计并试制了镗杆结构。通过冲击试验研究表明,直径为5 mm、填充率为70%的硬质合金颗粒可实现19.386%的阻尼比,具有出色的减振能力,可能降低镗削振动的可能性。接着,设置了实验以探究其在7075铝合金深孔镗削过程中的减振性能。为了更明显地观察,采用了恶劣的工作条件进行实验,以获取镗杆头部的时间域振动信号以及工件的表面形貌和粗糙度值。通过比较不同实验结果,发现与普通镗杆相比,设计的镗杆在两组实验中可将最大振动幅度降低高达81.01%,表面粗糙度值降低高达47.09%,证明了设计的镗杆能有效减少振动。本研究可为该材料的加工提供一些有价值的见解。

关键词:7075铝合金;镗杆;减振;颗粒阻尼